# A13 Degradation of SiC/SiC Ceramic Matrix Composite (CMC) at High Temperature Environments

高温環境における **SiC / SiC** セラミック基複合材料（**CMC**）の劣化

アミット パテル（東大・院），佐藤 英一 (JAXA)

Amit Patel (The University of Tokyo), Eiichi Sato (JAXA)

## 1. Introduction

SiC fiber-reinforced SiC Ceramic Matrix Composite (SiC/SiC CMC) is one of the newly developed composites from the past few decades and has shown strong contender with conventional superalloys which can be used for high-temperature applications such as various components of advance aircraft engines eg. turbine blades, vanes, shrouds, etc. [1]. With the use of these CMCs, we have certain advantages such as lightweight helpful in energy saving, less cooling air increasing fuel efficiency, high-temperature tolerance and so on.

One such important component made of SiC/SiC CMC is the combustion liner, which experiences high thermal gradients when the hot airflow passes through the combustion chamber of a jet engine. During this process, the liner is thermally expanded and bent due to the temperature gradients and causes compressive load on the supporting structure. The supporting part has structure discontinuity that results in inconsistent fibers distribution in some regions where high stresses are concentrated locally. These high-stress concentration regions are more prone to damage and fracture when cyclic loads are applied. Thus, the inhomogeneous temperature distribution along with cyclic compressive stresses leads to fatigue damage in the discontinuous, stress-concentrated part of the SiC/SiC CMC component. Previous studies have shown that fatigue behavior is severely affected by high temperatures and humid environments [2]. However, the prediction of fatigue damage initiation and growth in SiC/SiC CMC at high temperatures is much more complex as well as challenging as compared to room temperature. Hence further studies are still required as it involves multiple active damage mechanisms such as fiber fracture, matrix micro-cracking, fiber buckling, delamination, etc [3]. These issues are very critical and need to be solved for the application point of view.

However, the experimental tests at high temperatures consume lots of time and also cost-ineffective. So, a new approach is the application of multi-scale modeling. In this modeling, a micromechanics based approach has been used to understand the composite behavior at the constituent level such as matrix and fiber [4]. The set of two commercially available software namely Genoa and MCQ (AlphaSTAR Co.) are capable of estimating fracture and damage evolution from the ply to elemental level incorporating defects as well as composite architectures.

Hence, our main aim is to study the degradation behavior in high stress-concentrated regions of SiC/SiC CMC component due to fatigue at high-temperature environments using experimental as well as simulation route. This study will help to understand the key failure and damage mechanism as it still needs to fully understand these materials in order to further improve the properties.

## 2. Experimental Methods

The material used in the present study consists of SiC fiber-reinforced in CVI and PIP processed SiC matrix with BN as the interface. This SiC/SiC CMC component also has structure discontinuity as shown in Fig. 1. The sample is 25 mm long, 5 mm wide with thickness varies from 1 mm to 2 mm through the length. The compression test was done at 1100°C. The as-received sample was kept inside the heating furnace and heated up to 1100°C. The compression test was then performed in stroke control at a constant displacement rate of 0.2 mm/min.

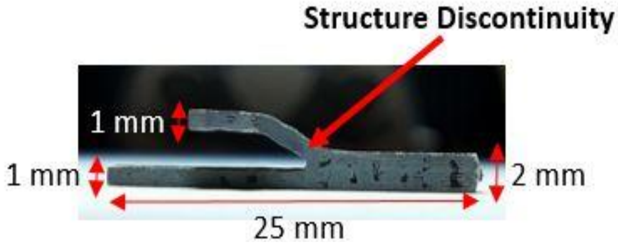

Fig.1 SiC/SiC CMC component

Finite Element modeling was done using FE software to study the stress distribution of the sample and to obtain the conditions for the fatigue tests. The preliminary fatigue tests were done at 1100°C at different force values 25 N, 30 N, 35 N and 40 N. The broken specimen was then observed in an optical microscope and SEM.

Initial calibration of input properties of the SiC/SiC CMC was also done using MCQ ceramic software. The software uses various experimental unidirectional ply properties to calculate the calibrated constituent fiber and matrix properties which are further utilized to obtain final calibrated SiC/SiC CMC component properties.

## 3. Results and Discussion

### *3.1 As-received specimen microstructure*

The SEM cross-sectional view of the as-received specimen is shown in Fig.2. It is observed that the sample contains CVI processed SiC fibers having an average diameter of 10 μm which are coated with a BN layer of thickness approximately 0.15 μm. The matrix is comprised of SiC which is first

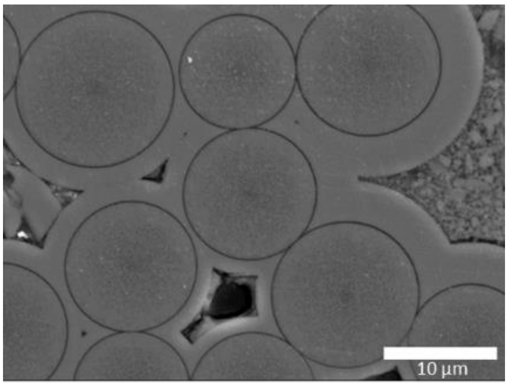

Fig.2 SEM cross sectional image of SiC/SiC CMC

processed by CVI and then a series of PIP cycles. However, the material also includes small pores that form during the manufacturing process.

*3.2 Compression test at 1100°C*

Fig. 3 shows the force vs cross-head displacement curve at 1100°C. It is observed that material withstand the maximum force of 47 N with a displacement of approximately 1.22 mm. This force value corresponds to the von Mises stress value of 530 MPa calculated by Finite Element analysis. From the graph, it is concluded that when the maximum force was reached, the first matrix micro-crack initiated followed by load transfer to the fiber where the sample started failing with continuously decreasing force until the final fracture of the specimen occurs.

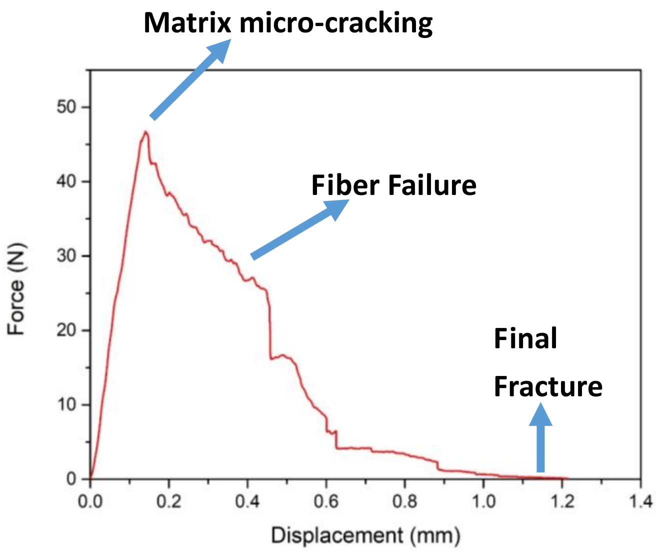


Fig. 3 Force vs cross-head displacement at 1100°C

Fig. 4(a) shows the crack propagation after the compression test in the fractured specimen. The crack was propagated (white dashed line) perpendicular to the force applied and restricted close to the surface of the sample. The microstructure reveals that the specimen failed in the shear manner (white arrows) as the tensile stresses generated only at the sample surface when the compressive force was applied. The various toughening mechanism such as fiber pullout (Fig. 4(b)) and crack deflection at the fiber/matrix interface (red dashed line in Fig. 4(c)) are also observed. The interface is one of the very important constituents in the fiber-reinforced CMCs. When the crack initiates from the SiC matrix and propagated towards the fiber, the BN interface tries to deflect the crack in order to delay the failure. Fiber pullout is also the indications of slow failure where fibers are pullout from the matrix without being fracture when the force is applied.

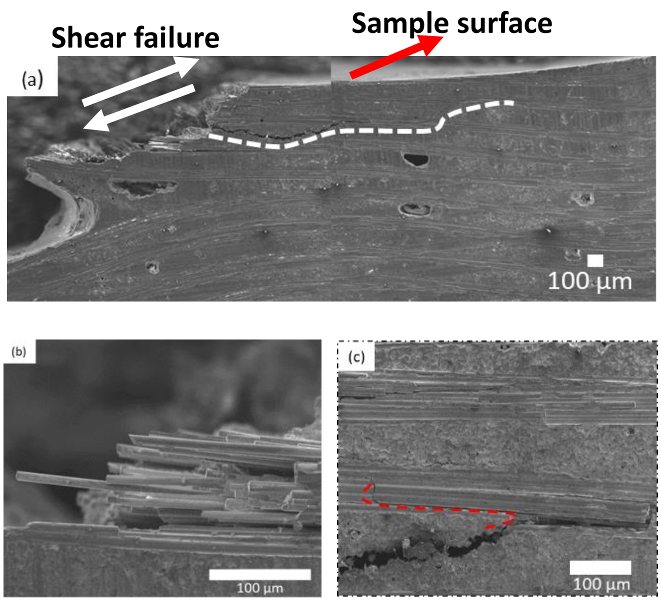


Fig. 4 SEM fracture microstructures after 1100°C compression test showing (a) crack propagation, (b) fiber pullout and (c) crack deflection

*3.3 Fatigue test at 1100°C*

The preliminary fatigue tests were done at three different load values 25, 30, 35 and 40 N with 1000 cycles for each load value at 1100°C. The apparent stiffness vs the number of fatigue cycles for different load values is shown in Fig. 5. It is noticed that the 25 N fatigue test shows higher apparent stiffness value as compared to 30 N and larger load values fatigue tests.

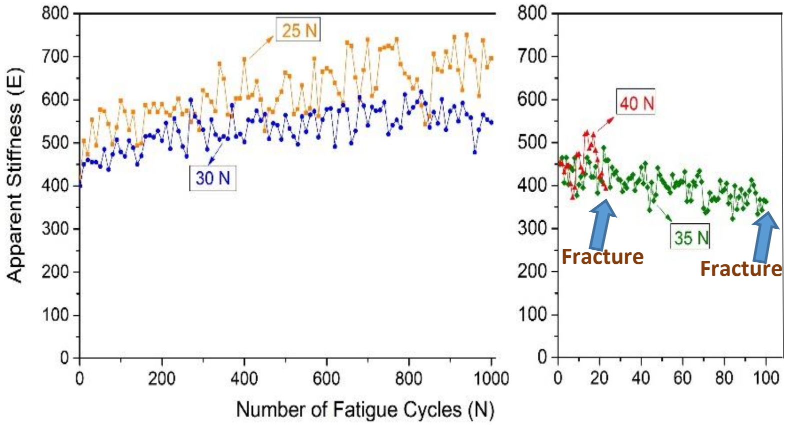


Fig.5 Apparent Stiffness vs Number of Fatigue cycles

The overall stiffness almost remains constant throughout 1000 cycles for 25 and 30 N; however, the material failed at higher load values of 35 and 40 N at the 100th and 23rd cycles, respectively. Since the specimen fractured without sufficient plastic deformation, it is concluded that specimen fracture in a brittle manner. As the stress value increases, oxygen from the air penetrate through the matrix micro-cracks and degrades the BN interface. The continuous degradation of the BN interface further allows the cracks to propagate into the fiber until the final failure of the component occurs. It is also worth mentioning that the fracture-initiation region also dependent on the actual shape and design of the present SiC/SiC CMC component as failure occurs in the structure discontinuous high-stress state region.

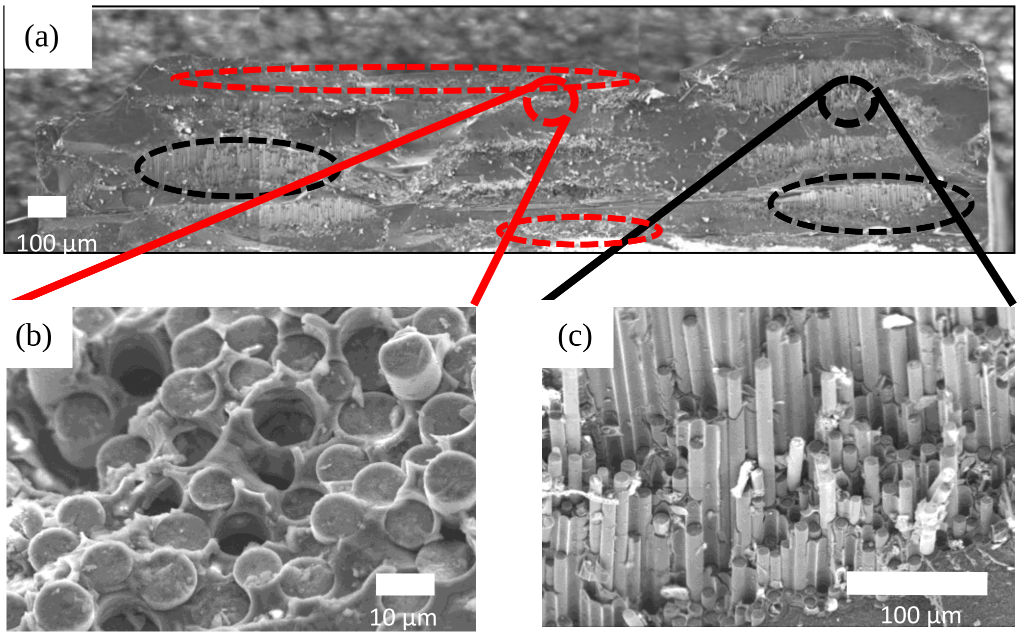


Fig. 6 SEM microstructures after 40 N fatigue test at 1100C showing (a) Fracture surface, (b) Brittle fracture region and (c) Fiber pullout region

The Fig. 6(a) show fracture microstructure of 40 N fatigue sample. It is observed that the microstructure consists of two different regions: one with brittle fracture with no fiber pullout region and another with significant fiber pullout region as shown in Fig. 6(b) and Fig. 6(c), respectively. From Fig. 6(b), it can be concluded that the fiber/matrix interface is severely degraded with increasing fatigue cycles at 1100°C. Various reactions are activated at high temperatures such as the formation of boria ($B_2O_3$) due to BN interface degradation and silica ($SiO_2$) from SiC oxidation. The silica and boria are then reacting together to form borosilicate glass until all the BN interface gradually consumes [6]. On the contrary, some regions are a less affected and hence considerable amount of fiber pullout is observed (Fig. 6(c)). This similar phenomenon is also reported by Ruggles-Wrenn et al. [1,5].

### *3.4 Calibration using MCQ Ceramics*

In order to proceed with simulation, calibration of material constant is one of the important steps. Initial calibration was done using MCQ Ceramic software. Calibration input values are Fiber Volume Ratio, Void Volume Ratio, fiber and matrix modulus including five ASTM standard test ply data. The software uses longitudinal and transverse mechanical properties to calculate constituent fiber and matrix properties respectively.

Table 1. Various mechanical properties of SiC/SiC CMC component obtained by simulation

| ***Mechanical Properties*** | ***Simulation Output Values*** | ***Unit*** |
|---|---|---|
| Young’s Modulus in X-axis (E11) | 266719 | MPa |
| Young’s Modulus in Y-axis (E22) | 140000 | MPa |
| Young’s Modulus in Z-axis (E33) | 140000 | MPa |
| Shear Modulus in XY axis (G12) | 90000 | MPa |
| Shear Modulus in XZ axis (G13) | 90000 | MPa |
| Shear Modulus in YZ axis (G23) | 65640 | MPa |
| Tensile Strength in X-axis (S11T) | 215 | MPa |
| Compressive Strength in X-axis (S11C) | 622 | MPa |
| Tensile Strength in Y-axis (S22T) | 150.6 | MPa |
| Compressive Strength in Y-axis (S22C) | 435.8 | MPa |
| Tensile Strength in Z-axis (S33T) | 150.6 | MPa |
| Compressive Strength in Z-axis (S33C) | 435.8 | MPa |
| Shear Strength in XY axis (S12) | 41.2 | MPa |
| Shear Strength in YZ axis (S23) | 55.7 | MPa |
| Shear Strength in XZ axis (S13) | 41.2 | MPa |

Using these constituent's calibrated properties and with the help of MCQ Ceramics by default ply mechanics option, the final ply mechanical properties are obtained as shown in Table.1. However, the present simulated results still need to be verified with the actual experimental test data. Nonetheless, these calibrated results will be further used for advance finite element based software Genoa which can able to predict the root cause behind the failure of the SiC/SiC component.

## 4. Conclusion

In the present work, the compression and fatigue tests of the SiC/SiC CMC component were done at 1100°C. Microstructure after compression test show various toughening mechanisms. The overall stiffness remains constant for 25 and 30 N signifies elastic deformation. There is no gradual deformation before specimen fracture even at a higher load (35 and 40 N) values which signify sudden failure. The fracture microstructure is, however, not homogeneous and consists of brittle and fiber pullout regions both. Ply properties of the SiC/SiC CMC component were obtained using MCQ Ceramics software.

The failure and degradation mechanisms due to fatigue in the localized high-stress regions of the SiC/SiC CMC component are still not clear at high-temperatures. A detailed study at the micro-level is still needed. This will be achieved by using experimental and software-based multi-scale progressive failure analysis simultaneously.

## References

[1] Ruggles-Wrenn, M.B. et al, Int. J. Fatigue, 47, (2013) 154-160.
[2] Zhu, S et al, Compos. Sci. Technol. 59, (1999) 833-851.
[3] Arnold, S.M. et al, 58th AIAA/ASCE/AHS/ASC Structures, Structural Dynamics, and Materials Conference, (2017) 1-21.
[4] DorMohammdi, S. et al, J. Compos. Mater. 51, (2017) 2181-2202.
[5] Ruggles-Wrenn, M.B. et al, Int. J. Appl. Ceram. Technol. 15, (2018) 3–15.
[6] Opila, E.J. et al, Int. J. Appl. Ceram. Technol. 13, (2016) 434-442.